AIAA JOURNAL
Vol. 31, No. 4, April 1993

Refined Shear Deformation Theory of Laminated Shells

Hung-Sying Jing* and Kuan-Goang Tzeng†
National Cheng Kung University, Tainan, Taiwan 70101, Republic of China

This paper establishes a refined approach for analyzing the effect of shear deformation in thick laminated anisotropic shells using a mixed formulation based on the functional proposed by Jing and Liao. The displacement field uses a zigzag function in addition to the Reissner-Mindlin type in-plane displacements and a constant transverse deflection. The effect of transverse shear deformation is included through an independently assumed transverse shear stress field. The initial curvature effect, which should not be neglected in thick shells, is included in the strain-displacement relations, stress resultants, and the assumed shear stress field. The governing equations are obtained by taking variations of the functional with respect to the displacements and transverse shear. The equations of motion of a general shell are given. Typical examples of thick laminated cross-ply cylindrical panels under cylindrical bending are given to illustrate the accuracy of the present refinement. From the examples investigated, it is concluded that the present theory can supply, with only seven equations, reasonably good results.

Introduction

FIBER-REINFORCED composites have been widely used in different industries because of their low weight and high strength. Among the different kinds of applications, the most important are laminated plates and shells. To be able to use composites with confidence, many researchers have developed theories to predict accurately their behavior under static and dynamic loadings. Up until now, most of the effort was concentrated on the laminated plates. Some instructive review articles can be found in the literature.[1-4] For shells, more and more studies have been made in recent years. The most general approach used in the literature is that which uses the principle of virtual work in conjunction with a pre-assumed displacement field. Derived from thin shell theory, the classical lamination theories for shells based on Kirchoff-Love postulates are adequate to predict the gross response of relatively thin laminates. A good survey of the different classical lamination theories can be found in the work of Naghdi[5] and Ambartsumyan.[6]

Owing to the high ratios of in-plane Young's modulus to transverse shear modulus of the most used composite materials, the influence of transverse shear deformation, which is not included in the classical lamination theories, cannot be neglected in certain cases. Also, when the laminates become thicker, the transverse shear effect has to be incorporated. As a result, numerous first-order and higher order shear deformation theories have been proposed for multilayered anisotropic shells.[7-10] By satisfying zero shear strains on the top and bottom surfaces, alternate higher order theories have been proposed for laminated shells.[11,12] Recently, Noor and Burton[13] summarized the research on the shear deformation theories for multilayered composite shells.

For the analysis of thick shells, in addition to the transverse shear deformation, the initial curvature effect also has to be considered, as indicated by Voyiadjis and Shi[14] for isotropic materials. In shell structure, the curvature for each parallel surface through the thickness of the shell is different. Therefore, the curvature of a surface located at a distance z from middle surface, whose curvature is $1/R$, is $1/[R(1+z/R)]$. To consider the initial curvature effect, the term $1+z/R$ has to be included. The importance of this effect is obvious when z/R is of the same order as 1. The incorporation of the initial curvature results in nonlinear distribution for the in-plane stresses along the thickness and unsymmetric stress resultants. Both of these are essential features of thick shells and should not be ignored for an accurate and reliable thick shell theory.

The aforementioned theories, classified as displacement-based theories, will in general violate the condition of traction continuity at the layer interfaces unless they employ specially designed displacement fields.[15,16] To overcome this drawback, other types of theories[17,18] were proposed, based on either Reissner's[19] mixed variational principle or the functional of Jing and Liao.[20] The survey of the analysis of multilayered composite shells using Reissner's mixed variational principle was done by Grigolyuk and Kulikov.[21] Jing and Liao's functional, modified from the Hellinger-Reissner principle by separating the stress field into a flexural part and a transverse shear part and leaving only displacements and transverse shear stresses as independent variables, has been used to analyze laminated plates with satisfactory accuracy. These analyses showed that with independently assumed transverse stresses or shear, instead of using displacements only, it is more accurate to consider shear effect. Although Reissner's and Jing and Liao's functionals are similar, they are not identical. The difference between the laminated plate theories derived from these two functionals was studied by Jing and Tzeng.[22]

Although the aforementioned shear deformation theories can yield reasonably good results for deflections, vibration frequencies, and buckling loads, they do not accurately predict through-thickness distributions of deformations and stresses. From studies for laminated plates, it was found that the zigzag displacement field suggested by Murakami[17] can improve the in-plane responses even better than most higher order theories. Consequently, in the present study, this type of displacement field, combined with Jing and Liao's functional, is extended to the analysis of thick laminated anisotropic shells to include the effect of shear deformation. In the present refinement, the exact three-dimensional elasticity is used to formulate the strain-displacement relations instead of using power series[23,24] to incorporate the initial curvature effect. Moreover, the same effect is also included in the stress resultants. In addition to the displacement field of the Murakami type, two transverse shear stresses are assumed a priori. The interface traction continuity condition and traction boundary conditions on the outer surfaces can thus be satisfied without difficulty. After performing the stationary operation of the functional, the resulting governing equations will include the equations of motion, compatibility of transverse shear, and consistent boundary conditions. The numerical

Received March 17, 1992; revision received Aug. 4, 1992; accepted for publication Aug. 14, 1992.

*Professor, Institute of Aeronautics and Astronautics.

†Graduate Student, Institute of Aeronautics and Astronautics.

results presented here for the laminated cross-ply circular cylindrical shell panels are compared with three-dimensional elasticity solutions[25] to show the accuracy of this refined mixed approach.

Theoretical Development

The curvilinear orthogonal coordinates (ξ_1, ξ_2, ξ_3) of the shell are introduced. Here $\xi_3 = 0$ represents a surface defined by (ξ_1, ξ_2) coinciding with the lines of principal curvature of the middle surface. The ξ_3 is defined to be along the straight line normal to the middle surface. Under this definition, the length of the linear element is

$$dS^2 = A_1^2(1 + k_1\xi_3)^2\, d\xi_1^2 + A_2^2(1 + K_2\xi_3)^2\, d\xi_2^2 + d\xi_3^2 \tag{1}$$

and the element of volume is

$$dV = A_1A_2(1 + k_1\xi_3)(1 + k_2\xi_3)\, d\xi_1\, d\xi_2\, d\xi_3 \tag{2}$$

where $A_\alpha = A_\alpha(\xi_1, \xi_2)$ are coefficients of the first quadratic form of the middle surface, and $k_\alpha = k_\alpha\,(\xi_1, \xi_2)$ are principal curvatures of the middle surface along the lines $\xi_2 =$ const, $\xi_1 =$ const, respectively. The area of an infinitesimal rectangle on edge surface S_e is

$$dS_e = H(\xi_3)\, d\xi_3\, ds_l \tag{3}$$

where

$$H(\xi_3) = \{[\nu_2(1 + k_1\xi_3)]^2 + [\nu_1(1 + k_2\xi_3)]^2\}^{1/2}$$

In the previous formula, ν_1 and ν_2 are the direction cosines of the curve C, which is the intersection of the middle surface and edge surface S_e, and s_l is measured along the curve C.

Consider a laminated composite shell consisting of N perfectly bonded homogeneous anisotropic elastic layers whose principal axes coincide with curvilinear orthogonal coordinates ξ_1, ξ_2, and ξ_3. Each layer of the composite has one plane of elastic symmetry perpendicular to the thickness direction. In the following derivation, $(\;)^{(k)}$, $k = 1, 2, \ldots, N$, represents the quantities corresponding to the kth layer. The thickness of the kth layer is denoted by h_k, and h is the total thickness of the shell, as shown in Fig. 1. Unless otherwise stated, the common Cartesian indicial notation is used where Latin and Greek indices range from 1 to 3 and 1 to 2, respectively. Repeated indices do not denote the summation convention, and $(\;)_{,i}$ represents partial differentiation with respect to ξ_i. For simplicity, a subscript π is introduced. Its value is 1 when $\alpha = 2$ and 2 when $\alpha = 1$.

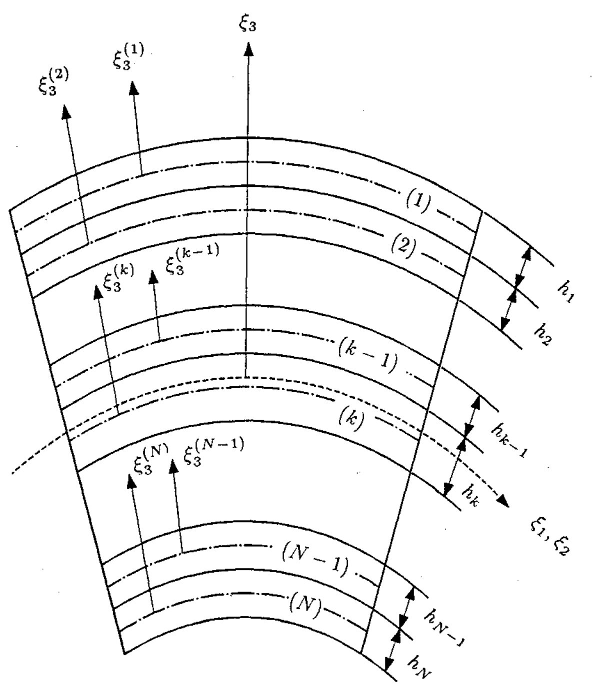

Fig. 1 Shell coordinates, geometry, and lamination.

The strain-displacement relations of the kth layer, derived from three-dimensional elasticity, including the initial curvature effect, is of the form

$$e_{\alpha\alpha}^{(k)} = \frac{1}{1 + k_\alpha\xi_3}\left[\frac{u_{\alpha,\alpha}^{(k)}}{A_\alpha} + \frac{A_{\alpha,\pi}u_\pi^{(k)}}{A_1A_2} + k_\alpha u_3^{(k)}\right] \tag{4a}$$

$$e_{12}^{(k)} = \frac{1}{1 + k_1\xi_3}\left[\frac{u_{2,1}^{(k)}}{A_1} - \frac{A_{1,2}u_1^{(k)}}{A_1A_2}\right] + \frac{1}{1 + k_2\xi_3}\left[\frac{u_{1,2}^{(k)}}{A_2} - \frac{A_{2,1}u_2^{(k)}}{A_1A_2}\right] \tag{4b}$$

$$e_{33}^{(k)} = u_{3,3}^{(k)} \tag{4c}$$

$$e_{\alpha 3}^{(k)} = \frac{1}{1 + k_\alpha\xi_3}\left[\frac{u_{3,\alpha}^{(k)}}{A_\alpha} - k_\alpha u_\alpha^{(k)}\right] + u_{\alpha,3}^{(k)} \tag{4d}$$

Having one plane of elastic symmetry, the constitutive equations of the kth layer can be separated into two equations and stated as

$$\begin{Bmatrix}\sigma_{11}\\ \sigma_{22}\\ \sigma_{33}\\ \sigma_{12}\end{Bmatrix}^{(k)} = \begin{bmatrix} C_{11} & C_{12} & C_{13} & C_{16}\\ C_{21} & C_{22} & C_{23} & C_{26}\\ C_{31} & C_{32} & C_{33} & C_{36}\\ C_{16} & C_{26} & C_{36} & C_{66}\end{bmatrix}^{(k)} \begin{Bmatrix} e_{11}\\ e_{22}\\ e_{33}\\ e_{12}\end{Bmatrix}^{(k)} \tag{5a}$$

$$\begin{Bmatrix} e_{13}\\ e_{23}\end{Bmatrix}^{(k)} = \begin{bmatrix} S_{11} & S_{12}\\ S_{12} & S_{22}\end{bmatrix}^{(k)} \begin{Bmatrix}\tau_{13}\\ \tau_{23}\end{Bmatrix}^{(k)} \tag{5b}$$

where C_{ij} and S_{ij} stand for the elastic moduli and compliance.

In the present theoretical development, a displacement field proposed by Murakami, having continuous piecewise linear in-plane displacements and a constant transverse deflection through the shell thickness is employed to formulate the mixed theory. The displacement field is expressed as follows:

$$u_\alpha^{(k)}(\xi_1, \xi_2, \xi_3) = U_\alpha(\xi_1, \xi_2) + \xi_3\Psi_\alpha(\xi_1, \xi_2) + (-1)^k\frac{2}{h_k}\,\xi_3^{(k)}S_\alpha(\xi_1, \xi_2) \tag{6a}$$

$$u_3^{(k)}(\xi_1, \xi_2, \xi_3) = U_3(\xi_1, \xi_2) \tag{6b}$$

where

$$\xi_3^{(k)} = \xi_3 - \xi_{30}^{(k)}, \qquad \frac{-h_k}{2} \le \xi_3^{(k)} \le \frac{h_k}{2}$$

represents a local ξ_3 coordinate with the origin at the center of the kth layer: $\xi_{30}^{(k)}$. It should be noted that there are seven independent variables U_i, Ψ_α, and S_α in the previous displacement field, regardless of the number of layers.

The transverse shear stresses are assumed as

$$\tau_{\alpha 3}^{(k)} = \frac{Q_\alpha^{(k)}f_q^{(k)}}{1 + k_\pi^{(k)}\xi_3^{(k)}} + p_1^{(k)}T_\alpha^{(k-1)} + p_2^{(k)}T_\alpha^{(k)} \tag{7}$$

where

$$f_q^{(k)} = \frac{3}{2h_k}(1 - 4\eta^2), \qquad p_\alpha^{(k)} = (-1)^{\alpha+1}\eta + 0.5$$

$$k_\alpha^{(k)} = \frac{1}{R_\alpha + \xi_{30}^{(k)}}, \qquad \eta = \frac{\xi_3^{(k)}}{h_k}$$

and R_α denotes the principal radii of the coordinate lines on the middle surface. In Eq. (7), $Q_\alpha^{(k)}$ represents the parabolic part, with the initial curvature effect of shear force in α

direction of the kth layer. $T_\alpha^{(k)}$ is the value of the transverse shear in the α direction and at the kth interface. The assumed transverse shear stress is composed of three parts. They are one parabolic term, including initial curvature effect, and two linear terms. Of the two linear terms, one is from the contribution of the traction at the upper surface whereas the other is from the lower surface. With this type of assumed stresses, the different kinds of transverse shear distributions in laminated shells, as long as these are piecewise parabolic, can all be modeled with satisfactory accuracy. It should be noted here that the transverse shear stresses satisfy the requirements

$$\tau_{3\alpha}^{(k)} = \tau_{3\alpha}^{(k+1)} \qquad k = 1, 2, \ldots, N-1 \tag{8}$$

which are the conditions of traction continuity at the layer interfaces, and

$$\tau_{3\alpha}^{(1)} = T_\alpha^{+} \qquad \text{at} \qquad \xi_3 = \frac{h}{2} \tag{9a}$$

$$\tau_{3\alpha}^{(N)} = T_\alpha^{-} \qquad \text{at} \qquad \xi_3 = -\frac{h}{2} \tag{9b}$$

Of course, T_α^+ and T_α^- are the prescribed tractions on the top and bottom surfaces in the α direction. Using Eqs. (7) and (9), the traction boundary conditions are satisfied, i.e., $T_\alpha^{(0)} = T_\alpha^+$, and $T_\alpha^{(N)} = T_\alpha^-$. In the present theory, only two transverse shear components are assumed, unlike Reissner's formulation in which transverse normal as well as transverse shear have to be assumed a priori. It makes the derivation presented here much more simple as can be seen in the previous studies for plates.[22] In fact, unless the value of the deflection wavelength is close to that of the thickness, the contribution from the transverse normal stress can usually be neglected.

The purpose of this paper is to develop a mixed theory that accurately includes the effect of transverse shear deformation. To complete this analysis, Jing and Liao's mixed variational principle is applied to N-layered composite laminated shells whose middle surfaces occupy domain A in the ξ_1 and ξ_2 directions, i.e.,

$$\begin{aligned}
&\int_{t_0}^{t_1}\left[\iint_A\left(\sum_{k=1}^{N}\int_{\Omega^{(k)}}\{\delta e_{ij}^{(k)}\sigma_{ij}^{(k)} + \delta\tau_{13}^{(k)}[u_{1,3}^{(k)} + u_{3,1}^{(k)}\right.\right.\\
&\quad - S_{11}^{(k)}\tau_{13}^{(k)} - S_{12}^{(k)}\tau_{23}^{(k)}] + \delta\tau_{23}^{(k)}[u_{2,3}^{(k)} + u_{3,2}^{(k)} - S_{12}^{(k)}\tau_{13}^{(k)} - S_{22}^{(k)}\tau_{23}^{(k)}]\\
&\quad \left.\left. - \rho^{(k)}\dot{u}_i^{(k)}\delta\dot{u}_i^{(k)}\}(1+k_1\xi_3)(1+k_2\xi_3)\,\mathrm{d}\xi_3\right)A_1A_2\,\mathrm{d}\xi_1\,\mathrm{d}\xi_2\right]\mathrm{d}t\\
&= \int_{t_0}^{t_1}\left\{\iint_A\left[\sum_{k=1}^{N}\int_{\Omega^{(k)}}\delta u_i^{(k)}f_i^{(k)}(1+k_1\xi_3)(1+k_2\xi_3)\,\mathrm{d}\xi_3\right.\right.\\
&\quad + \delta u_i^{(1)}\left(\xi_1, \xi_2, \frac{h}{2}\right)T_i^{+}\left(1+\frac{k_1h}{2}\right)\left(1+\frac{k_2h}{2}\right)\\
&\quad \left. + \delta u_i^{(N)}\left(\xi_1, \xi_2, -\frac{h}{2}\right)T_i^{-}\left(1-\frac{k_1h}{2}\right)\left(1-\frac{k_2h}{2}\right)\right]\\
&\quad \times A_1A_2\,\mathrm{d}\xi_1\,\mathrm{d}\xi_2\\
&\quad \left. + \int_{\partial C_p}\left[\sum_{k=1}^{N}\int_{\Omega^{(k)}}\delta u_i^{(k)}\bar{p}_iH(\xi_3)\,\mathrm{d}\xi_3\right]\mathrm{d}s_l\right\}\mathrm{d}t
\end{aligned} \tag{10}$$

where repeated indices denote the summation convention, ∂C_p denotes the part of traction prescribed on curve C, $\bar{p}_i$ stands for prescribed traction in i direction, $\Omega^{(k)}$ is the ξ_3 domain occupied by the kth layer, $f_i^{(k)}$ is the body force of the kth layer in i direction, and $\rho^{(k)}$ is the density of the kth layer.

By introducing Eqs. (4), (6), and (7) into Eq. (10) and taking variation with respect to the independent variables U_i, Ψ_α, and S_α and the transverse shear, the following equations of motion, transverse shear compatibility, and boundary conditions are obtained.

Equations of motion:

$$\begin{aligned}
&(A_2N_{1\alpha})_{,1} + (A_1N_{2\alpha})_{,2} + (-1)^{\alpha}A_{2,1}N_{2\pi} + (-1)^{\alpha+1}A_{1,2}N_{1\pi}\\
&\quad + k_\alpha A_1A_2N_{\alpha3} + A_1A_2\left[B_\alpha^a + (T_\alpha^+ - T_\alpha^-)\left(1+\frac{k_1k_2h^2}{4}\right)\right.\\
&\quad \left. + (T_\alpha^+ + T_\alpha^-)\frac{(k_1+k_2)h}{2}\right]\\
&\quad = A_1A_2(I_1\ddot{U}_\alpha + I_2\ddot{\Psi}_\alpha + I_3\ddot{S}_\alpha)
\end{aligned} \tag{11a}$$

$$\begin{aligned}
&(A_2N_{13})_{,1} + (A_1N_{23})_{,2} - A_1A_2(k_1N_{11} + k_2N_{22})\\
&\quad + A_1A_2\left[B_3^a + (T_3^+ - T_3^-)\left(1+\frac{k_1k_2h^2}{4}\right)\right.\\
&\quad \left. + (T_3^+ + T_3^-)\frac{(k_1+k_2)h}{2}\right]\\
&\quad = A_1A_2I_3\ddot{U}_3
\end{aligned} \tag{11b}$$

$$\begin{aligned}
&(A_2M_{1\alpha})_{,1} + (A_1M_{2\alpha})_{,2} + (-1)^{\alpha}A_{2,1}M_{2\pi} + (-1)^{\alpha+1}A_{1,2}M_{1\pi}\\
&\quad - A_1A_2N_{\alpha3} + A_1A_2\left[B_\alpha^b + \frac{h}{2}(T_\alpha^+ - T_\alpha^-)\left(1+\frac{k_1k_2h^2}{4}\right)\right.\\
&\quad \left. + (T_\alpha^+ - T_\alpha^-)\frac{(k_1+k_2)h^2}{4}\right]\\
&\quad = A_1A_2(I_2\ddot{U}_\alpha + I_5\ddot{\Psi}_\alpha + I_4\ddot{S}_\alpha)
\end{aligned} \tag{11c}$$

$$\begin{aligned}
&(A_2L_{1\alpha})_{,1} + (A_1L_{2\alpha})_{,2} + (-1)^{\alpha}A_{2,1}L_{2\pi} + (-1)^{\alpha+1}A_{1,2}L_{1\pi}\\
&\quad - A_1A_2K_{\alpha3} + A_1A_2\left\{B_\alpha^c - [T_\alpha^+ - (-1)^NT_\alpha^-]\left(1+\frac{k_1k_2h^2}{4}\right)\right.\\
&\quad \left. + [T_\alpha^+ + (-1)^NT_\alpha^-]\frac{(k_1+k_2)h}{2}\right\}\\
&\quad = A_1A_2(I_3\ddot{U}_\alpha + I_5\ddot{\Psi}_\alpha + I_6\ddot{S}_\alpha)
\end{aligned} \tag{11d}$$

where the variables are defined as follows:

$$\begin{aligned}
(N_{\alpha\beta}, M_{\alpha\beta}, L_{\alpha\beta}) &= \sum_{k=1}^{N}\int_{\Omega^{(k)}}\sigma_{\alpha\beta}^{(k)}(1+k_\pi\xi_3)\left[1, \xi_3, (-1)^k\right.\\
&\quad \left.\times\frac{2}{h_k}\xi_3^{(k)}\right]\mathrm{d}\xi_3
\end{aligned} \tag{12a}$$

$$\begin{aligned}
(N_{\alpha3}, K_{\alpha3}) &= \sum_{k=1}^{N}\int_{\Omega^{(k)}}\tau_{\alpha3}^{(k)}(1+k_\pi\xi_3)\left[1, (-1)^k\right.\\
&\quad \left.\times\frac{2}{h_k}(1+k_\alpha\xi_{30}^{(k)})\right]\mathrm{d}\xi_3
\end{aligned} \tag{12b}$$

$$\begin{aligned}
(I_1, I_2, I_3, I_4, I_5, I_6) &= \sum_{k=1}^{N}\int_{\Omega^{(k)}}\rho^{(k)}\left[1, \xi_3(-1)^k\frac{2}{h_k}\xi_3^{(k)}, \xi_3^2,\right.\\
&\quad \left.(-1)^k\frac{2}{h_k}\xi_3\xi_3^{(k)}, \frac{4}{h_k^2}\xi_3^{(k)^2}\right](1+k_1\xi_3)(1+k_2\xi_3)\,\mathrm{d}\xi_3
\end{aligned} \tag{12c}$$

$$\begin{aligned}
(B_i^a, B_i^b, B_i^c) &= \sum_{k=1}^{N}\int_{\Omega^{(k)}}\left[1, \xi_3(-1)^k\frac{2}{h_k}\xi_3^{(k)}\right]\\
&\quad \times(1+k_1\xi_3)(1+k_2\xi_3)f_i^{(k)}\,\mathrm{d}\xi_3
\end{aligned} \tag{12d}$$

It should be noted that the initial curvature effect is included in the previous stress resultants. There are seven equations in total. The first two equations, (11a), imply the balance of the in-plane forces in ξ_1 and ξ_2 directions. The third equation, (11b), represents the force balance in the transverse direction.

Equations (11c) are moment equations. The last two equations, (11d), are equations of motion corresponding to the assumed zigzag displacement field.

Transverse shear compatibility:

$$Q_1^{(k)} + \left(\frac{S_{12}a_3}{S_{11}a_1}\right)^{(k)} Q_2^{(k)} + \left(\frac{b_1}{a_1}\right)^{(k)} T_1^{(k-1)} + \left(\frac{b_3}{a_1}\right)^{(k)} T_1^{(k)} + \left(\frac{S_{12}b_1}{S_{11}a_1}\right)^{(k)} T_2^{(k-1)} + \left(\frac{S_{12}b_3}{S_{11}a_1}\right)^{(k)} T_2^{(k)} = \left(\frac{e_1\gamma_1}{S_{11}a_1}\right)^{(k)} \tag{13a}$$

$$\begin{aligned}&[S_{11}^{(k+1)} b_1^{(k+1)} Q_1^{(k+1)} + S_{11}^{(k)} b_3^{(k)} Q_1^{(k)}] \\ &+ [S_{12}^{(k+1)} b_2^{(k+1)} Q_2^{(k+1)} + S_{12}^{(k)} b_4^{(k)} Q_2^{(k)}] \\ &+ \{S_{11}^{(k)} d_2^{(k)} T_1^{(k-1)} + [S_{11}^{(k+1)} d_1^{(k+1)} + S_{11}^{(k)} d_3^{(k)}] \\ &\times T_1^{(k)} + S_{11}^{(k+1)} d_2^{(k+1)} T_1^{(k+1)}\} + \{S_{12}^{(k)} d_2^{(k)} T_2^{(k-1)} \\ &+ [S_{12}^{(k+1)} d_1^{(k+1)} + S_{12}^{(k)} d_3^{(k)}] T_2^{(k)} + S_{12}^{(k+1)} d_2^{(k+1)} T_2^{(k+1)}\} \\ &= c_1^{(k+1)} \gamma_1^{(k+1)} + c_3^{(k)} \gamma_1^{(k)}\end{aligned} \tag{13b}$$

$$\left(\frac{S_{12}a_3}{S_{22}a_2}\right)^{(k)} Q_1^{(k)} + Q_2^{(k)} + \left(\frac{S_{12}b_2}{S_{22}a_2}\right)^{(k)} T_1^{(k-1)} + \left(\frac{S_{12}b_4}{S_{22}a_2}\right)^{(k)} T_1^{(k)} + \left(\frac{b_2}{a_2}\right)^{(k)} T_2^{(k-1)} + \left(\frac{b_4}{a_2}\right)^{(k)} T_2^{(k)} = \left(\frac{e_2\gamma_2}{S_{22}a_2}\right)^{(k)} \tag{13c}$$

$$\begin{aligned}&[S_{12}^{(k+1)} b_1^{(k+1)} Q_1^{(k+1)} + S_{12}^{(k)} b_3^{(k)} Q_1^{(k)}] \\ &+ [S_{22}^{(k+1)} b_2^{(k+1)} Q_2^{(k+1)} + S_{22}^{(k)} b_4^{(k)} Q_2^{(k)}] \\ &+ \{S_{12}^{(k)} d_2^{(k)} T_1^{(k-1)} + [S_{12}^{(k+1)} d_1^{(k+1)} + S_{12}^{(k)} d_3^{(k)}] \\ &\times T_1^{(k)} + S_{12}^{(k+1)} d_2^{(k+1)} T_1^{(k+1)}\} + \{S_{22}^{(k)} d_2^{(k)} T_2^{(k-1)} \\ &+ [S_{22}^{(k+1)} d_1^{(k+1)} + S_{22}^{(k)} d_3^{(k)}] T_2^{(k)} + S_{22}^{(k+1)} d_2^{(k+1)} T_2^{(k+1)}\} \\ &= c_2^{(k+1)} \gamma_2^{(k+1)} + c_4^{(k)} \gamma_2^{(k)}\end{aligned} \tag{13d}$$

where

$$\gamma_\alpha^{(k)} = \frac{U_{3,\alpha}}{A_\alpha} - k_\alpha U_\alpha + \Psi_\alpha + (-1)^k \frac{2}{h_k}[1 + k_\alpha \xi_{30}^{(k)}] S_\alpha$$

where $a_i^{(k)}$, $d_i^{(k)}$, $b_j^{(k)}$, $c_j^{(k)} (j = 1 \sim 4)$, and $e_\alpha^{(k)}$ are expressed in Eq. (A1). In Eqs. (13a) and (13c), k ranges from 1 to N, and in Eqs. (13b) and (13d), k ranges from 1 to $N-1$. The terms $Q_\alpha^{(k)}$ and $T_\alpha^{(k)}$ are expressed in terms of $\gamma_\alpha^{(k)}$ and $\gamma_\alpha^{(k+1)}$. Physically, Eqs. (13a–13d) represent compatibility of transverse shear. That is, they are the variational relations between transverse shear stresses and displacements.

Boundary conditions:

$$\text{Specify} \quad U_i \quad \text{or} \quad N_{\beta i}\nu_\beta \tag{14a}$$

$$\text{Specify} \quad \Psi_\alpha \quad \text{or} \quad M_{\beta\alpha}\nu_\beta \tag{14b}$$

$$\text{Specify} \quad S_\alpha \quad \text{or} \quad L_{\beta\alpha}\nu_\beta \tag{14c}$$

where repeated indices are the summation convention. The previous equations represent the displacement and force boundary conditions.

From Eqs. (4–6) and Eq. (12a), the in-plane stress resultants can be formulated as functions of U_i, Ψ_α, S_α, and their derivatives. On the other hand, with Eqs. (7), (8), and (12b), the transverse shear stress resultants can also be derived as functions of U_i, Ψ_α, and S_α. After substituting these equations into the equations of motion, Eqs. (11a–11g), and boundary conditions, Eqs. (14a–14c), a complete set of governing equations and the boundary conditions in terms of displacement variables can be formulated. If the external loading is further prescribed, it is then possible to find the solution of the resulting problem.

Cylindrical Bending of Laminated Cylindrical Panels

The coordinate system (ξ_1, ξ_2, ξ_3) is now replaced by the usual notation (x,y,z), in which $x = A_1 d\xi_1$ and $y = A_2 d\xi_2$. The panel is simply supported at the boundaries along $y = 0$ and $y = b$ and is infinitely long in the x direction, as shown in Fig. 2. The first fundamental form and curvatures of a circular cylindrical shell are

$$A_1 = 1, \qquad A_2 = R, \qquad k_1 = 0, \quad k_2 = \frac{1}{R} \tag{15}$$

where R is the mean radius of the cylindrical panel. The traction boundary conditions on the outer surfaces are

$$T_z^+ = q_0 \sin\frac{\pi y}{b}, \qquad T_z^- = T_y^+ = T_y^- = 0 \tag{16}$$

where $b = R\phi$. The cylindrical bending problem of laminated cross-ply cylindrical panels considered here is independent of the longitudinal coordinate x. The quantities U_x, Ψ_x, and S_x are zero. With Eqs. (15) and (16), the seven equations of equilibrium, Eqs. (11a–11g), can be reduced to

$$\begin{aligned}&N_{y,y} + \frac{N_{yz}}{R} = 0, \qquad N_{yz,y} - \frac{N_y}{R} + \left(1 + \frac{h}{2R}\right) q_0 \sin\frac{\pi y}{b} = 0 \\ &M_{y,y} - N_{yz} = 0, \qquad L_{y,y} - K_{yz} = 0\end{aligned} \tag{17}$$

The corresponding boundary conditions are

$$N_y = M_y = L_y = U_z = 0 \tag{18}$$

The simplified expressions for the stress resultants become

$$\begin{Bmatrix} N_y \\ M_y \\ L_y \end{Bmatrix} = \begin{bmatrix} G_{22} & F_{22} & E_{22} \\ F_{22} & P_{22} & Q_{22} \\ E_{22} & Q_{22} & Z_{22} \end{bmatrix} \begin{Bmatrix} U_{y,y} + U_z/R \\ \Psi_{y,y} \\ S_{y,y} \end{Bmatrix}$$

$$\begin{Bmatrix} N_{yz} \\ K_{yz} \end{Bmatrix} \begin{bmatrix} G_{11}^* & G_{12}^* \\ G_{21}^* & G_{22}^* \end{bmatrix} \begin{Bmatrix} U_{z,y} - U_y/R + \Psi_y \\ S_y \end{Bmatrix} \tag{19}$$

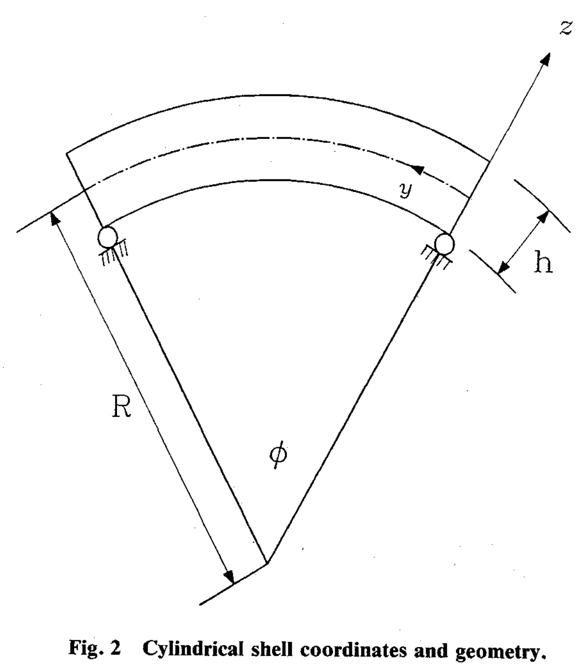

Fig. 2 Cylindrical shell coordinates and geometry.

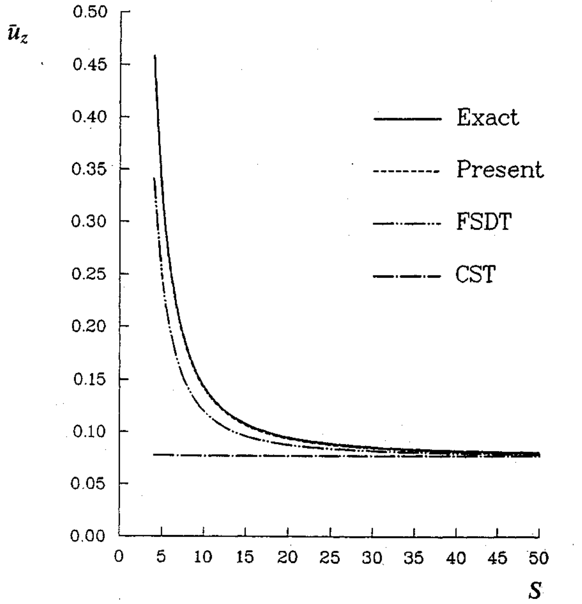

Fig. 3 Effect of S ratio on the deflection with $E_L/E_T = 25$.

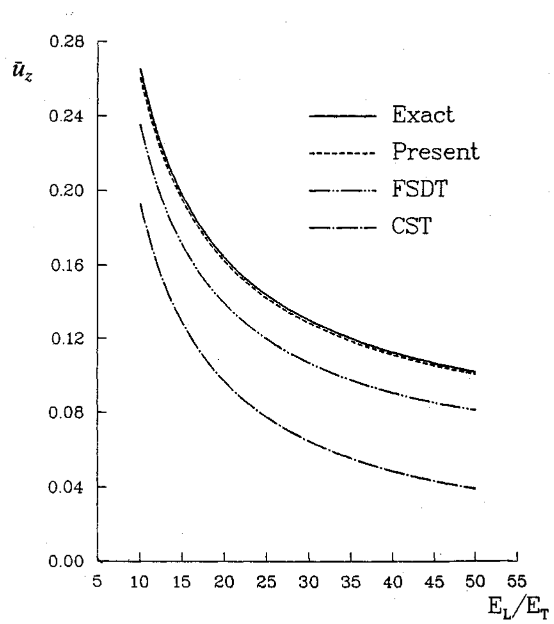

Fig. 4 Effect of material anisotropy on the transverse deflection with $S = 10$.

where

$$G_{22} = R\sum_{k=1}^{N} C_{22}^{(k)}\tilde{g}_0, \qquad F_{22} = R\sum_{k=1}^{N} C_{22}^{(k)}h_k(\tilde{g}_1 + c\tilde{g}_0)$$

$$E_{22} = 2R\sum_{k=1}^{N}(-1)^k C_{22}^{(k)}\tilde{g}_1$$
$$P_{22} = R\sum_{k=1}^{N} C_{22}^{(k)}h_k^2(\tilde{g}_2 + 2c\tilde{g}_1 + c^2\tilde{g}_0) \tag{20}$$

$$Q_{22} = 2R\sum_{k=1}^{N}(-1)^k C_{22}^{(k)}h_k(\tilde{g}_2 + c\tilde{g}_1), \quad Z_{22} = 4R\sum_{k=1}^{N} C_{22}^{(k)}\tilde{g}_2$$

and

$$G_{11}^* = \ell_1^T g_1 + m_1^T f_1, \qquad G_{12}^* = \ell_1^T g_2 + m_1^T f_2$$
$$G_{21}^* = \ell_2^T g_1 + m_2^T f_1, \qquad G_{22}^* = \ell_2^T g_2 + m_2^T f_2 \tag{21}$$

$$(f_1, f_2) = (F_1, A_1 - B_1)^{-1}(F_1 p_1 - q_1, F_1 p_2 - q_2)$$
$$(g_1, g_2) = (p_1 - A_1 f_1, p_2 - A_1 f_2)$$

where $c = z_0^{(k)}/h_k$. The constants $\tilde{g}_0$, $\tilde{g}_1$, and $\tilde{g}_2$ are listed in Eq. (A1a), and the matrices ℓ_α^T, m_α^T, A_1, B_1, F_1, p_α, and q_α are expressed in Eq. (A2).

Since the loading is of the sinusoidal type, by satisfying the boundary conditions, the Navier-type series solutions for static response can be given as

$$(U_y, \Psi_y, S_y) = (\tilde{U}_y, \tilde{\Psi}_y, \tilde{S}_y)\cos\frac{\pi y}{b}, \qquad U_z = \tilde{U}_z \sin\frac{\pi y}{b} \tag{22}$$

Substitution of Eqs. (19) and (22) into Eq. (17) yields a set of four linear algebraic equations in terms of the unknown constants $\tilde{U}_y$, $\tilde{U}_z$, $\tilde{\Psi}_y$, and $\tilde{S}_y$, which can be expressed in matrix form:

$$V\delta = F \tag{23}$$

where the column matrices $\delta^T = [\tilde{U}_y \ \tilde{U}_z \ \tilde{\Psi}_y \ \tilde{S}_y]$ and $F^T = [0 \ q_0(1 + h/2R) \ 0 \ 0]$. The components of matrix V are listed in Eq. (A3).

Numerical Examples

To assess the accuracy of this approach to the static analysis of a thick laminated panel, an example with the elasticity solution is used. For ease of comparison, the following laminae material properties, geometry, and loading condition are employed:

$$E_L = 25E_T, \quad G_{LT} = 0.5E_T, \quad G_{TT} = 0.2E_T, \quad \nu_{LT} = 0.25$$
$$\nu_{TT} = 0.49, \quad E_T = 1\times 10^6 \text{ psi},$$
$$b = \frac{10\pi}{3}\text{ in.}, \quad T_z^+ = q_0 \sin\frac{\pi y}{b} \tag{24}$$

where L denotes the direction parallel to the fibers, T the transverse direction, and ν_{LT} the Poisson ratio, measuring strain in the transverse direction under uniaxial normal stress.

The laminated shell under consideration is a three-layer [90 deg/ 0 deg/90 deg] infinitely long cylindrical shell with simply supported edges, and the loading is of a sinusoidal type. For comparison, the deflections and stresses are normalized as

$$\bar{\sigma}_y = \frac{1}{q_0 S^2}\sigma_y\left(\frac{b}{2}, z\right), \qquad \bar{\tau}_{yz} = \frac{1}{q_0 S}\tau_{yz}(0, z)$$

$$\bar{u}_y = \frac{100E_T}{q_0 S^3 h}u_y(0, z), \quad \bar{u}_z = \frac{10E_T}{q_0 S^4 h}u_z\left(\frac{b}{2}, 0\right) \tag{25}$$

$$S = \frac{R}{h}, \qquad \bar{z} = \frac{z}{h}$$

where u_y and u_z stand for displacements along the y and z directions. Figure 3 gives the comparisons of the transverse deflections from classical shell theory (CST), first-order shear deformation theory (FSDT), the present approach, and the exact theory. In this figure, the ratio S ranges from 4 to 50. The reason for choosing varied S is to assess the effect of shear deformation. As S decreases, the shear effect is more pronounced. As can be seen in this figure, in this range the present approach gives very good results when compared with the elasticity solutions.

Besides the thickness of laminated shells, the ratio E_L/E_T, which is the other parameter controlling the effect of shear deformation, is also used to evaluate the present approach. The comparisons are given in Fig. 4. In this case, $S = 10$ is used. The discrepancy between the present approach and the elasticity solution is not substantial. The studies with different

Table 1 Comparisons of nondimensionalized deflection and stresses for various theories vs exact

S	Theory	$\bar{u}_z(b/2, 0)$	$\bar{\sigma}_y(b/2, \pm h/2)$	$\bar{\tau}_{yz}(0, 0)$
4	Exact	0.458	− 1.360 − 1.772	0.476
	Present	0.459	1.205 − 1.550	0.511
	HSDT[a]	0.382	1.117 − 1.406	0.326
	FSDT[b]	0.342	0.732 − 0.824	0.225
	CST[c]	0.0781	0.732 − 0.824	—
10	Exact	0.144	0.898 − 0.993	0.525
	Present	0.142	0.870 − 0.96	0.574
	HSDT	0.128	0.829 − 0.88	0.340
	FSDT	0.120	0.759 − 0.796	0.225
	CST	0.0777	0.759 − 0.79	—
50	Exact	0.0808	0.784 − 0.800	0.525
	Present	0.0802	0.781 − 0.797	0.576
	HSDT	0.0796	0.774 − 0.789	0.328
	FSDT	0.0793	0.774 − 0.781	0.225
	CST	0.0776	0.774 − 0.781	—
100	Exact	0.0787	0.779 − 0.786	0.523
	Present	0.0780	0.778 − 0.786	0.574
	HSDT	0.0781	0.770 − 0.787	0.334
	FSDT	0.0780	0.776 − 0.779	0.225
	CST	0.0776	0.776 − 0.779	—

[a]HSDT: higher order shear deformation theory.[12]
[b]FSDT: first-order shear deformation theory.[9]
[c]CST: classical shell theory.

values of S, up to $S = 4$, have also been performed. The comparisons are all very similar to those shown in Fig. 4.

In addition to the deflection, the bending stress and transverse shear are also given in Table 1. Besides CST, FSDT, and the elasticity theory, results from higher order shear deformation theory[12] (HSDT) are also included for comparison. In their analysis, a special displacement field satisfying zero transverse shear on top and bottom surfaces of the shell is used. The results are from finite element analysis. In Table 1, the values of S used are 4, 10, 50, and 100. As shown in this table, the present approach generally gives better results than this higher order shear deformation theory.

To further evaluate the viability of the present approach, the through-thickness distributions of deformations and stresses are also analyzed and compared with other theories. Figure 5 gives displacements $\bar{u}_y$ along the circumferential direction for $S = 10$. This figure shows that the present approach gives results quite close to the elasticity solutions. Through-thickness stress $\bar{\sigma}_y$ along the circumferential direction from different theories are plotted in Fig. 6. Again, very good comparisons are shown between the elasticity and present approach. Because the results of $\bar{\sigma}_y$ from FSDT are identical to those from CST, they will not be shown in Figs. 6, 8, and 11. Figures 7 and 8 show the same comparisons but with different geometry. In this case, an $R/h = 4$ shell is used. The other parameters remain the same. Good comparisons between the present approach and the elasticity are maintained.

In many problems related to composites, the transverse shear stresses are very important. Figure 9 shows the through thickness transverse shear $\bar{\tau}_{yz}$. Since the traction-free conditions on the top and bottom surfaces and the continuity conditions along interfaces are satisfied in the assumed transverse shear fields, unreasonable discontinuity phenomena do not show up in the present approach. The comparison between the elasticity and the present approach is acceptable. Unfortunately, discrepancies can still be found along the interfaces. It should be noted here that the transverse shear stresses along the upper and lower interfaces differ. Without the initial curvature effect, the analysis from Dennis and Palazotti[12] obtained the same values along these two interfaces, as can be seen in Fig. 9. Since the initial curvature effect is included in the assumed transverse shear stress field [Eq. (7)], the same tendency as in the elasticity solution is revealed in the present

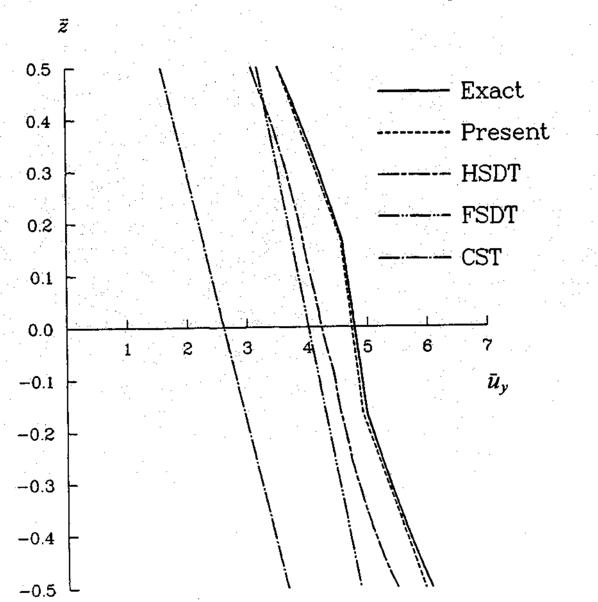

Fig. 5 Variation of circumferential displacement $\bar{u}_y(0, z)$ through laminated thickness of three-layer cross ply [90 deg/0 deg/90 deg] with $S = 10$.

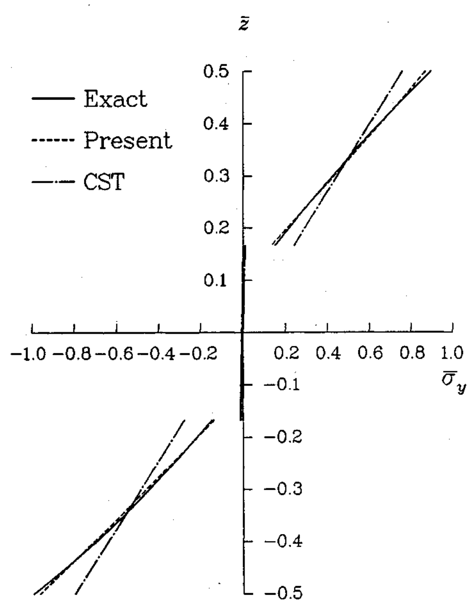

Fig. 6 Variation of circumferential stress $\bar{\sigma}_y(b/2, z)$ through laminated thickness of three-layer cross ply [90 deg/0 deg/90 deg] with $S = 10$.

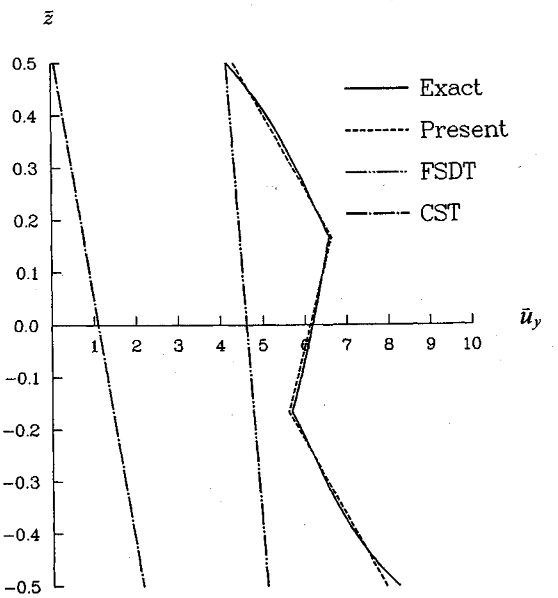

Fig. 7 Variation of circumferential displacement $\bar{u}_y(0, z)$ through laminated thickness of three-layer cross ply [90 deg/0 deg/90 deg] with $S = 4$.

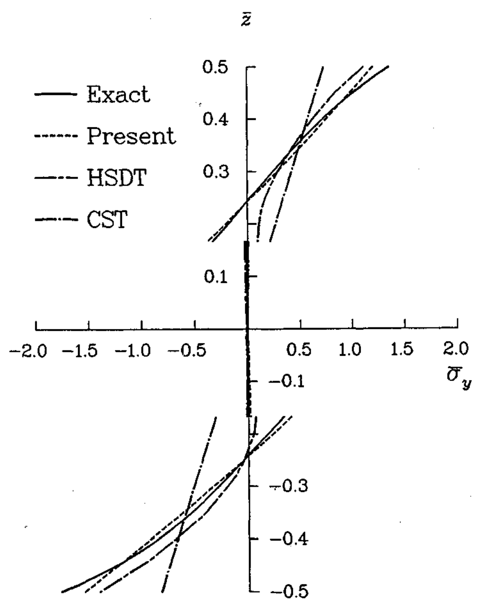

Fig. 8 Variation of circumferential stress $\bar{\sigma}_y(b/2, z)$ through laminated thickness of three-layer cross ply [90 deg/0 deg/90 deg] with $S = 4$.

analysis, suggesting that to incorporate the initial curvature effect is a must.

To further understand the behavior of the present approach, additional studies are done. Figures 10 and 11 show similar comparisons from different theories. The only difference is that the number of layers is increased to five and the stacking sequence is [90 deg/0 deg/90 deg/0 deg/90 deg]. In these figures, $S = 4$ is used. The displacement and in-plane stresses are compared with those from elasticity theory and again the results are acceptable.

From the previous analysis, the agreement between the present approach and the elasticity solution is shown to be acceptable. The reasons are thought to be as follows. The zigzag shape of displacement is a good displacement field to model through-thickness displacement. Also, the shape of assumed displacement is found to be very important to a successful modeling. The second reason is the mixed formulation. The assumed transverse shear field makes the shell more shear deformable, resulting in more chance of approaching the elasticity solution. The present study also found that the results of an analysis with an identical displacement field but without transverse shear are worse than those given in the previous figures. Mixed formulation does improve the performance of a theory to some extent. The third reason is thought to be due to the incorporation of the initial curvature effect in the present formulation. As the thickness increases, the term $(1 + z/R)$, usually neglected in most shell theories, becomes more important. The initial curvature effect is implanted in the strain-displacement relations, stress resultants, and the assumed transverse shear fields, contributing to the good comparison shown in the present study.

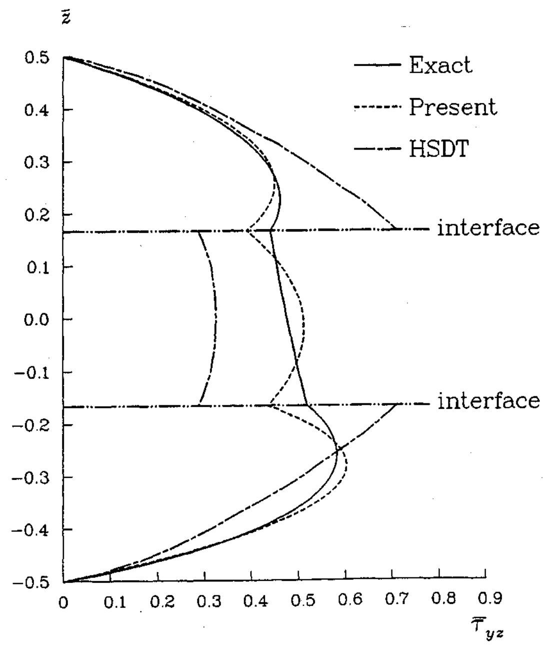

Fig. 9 Transverse shear stress distribution $\bar{\tau}_{yz}(0, z)$ through laminated thickness of five-layer cross ply [90 deg/0 deg/90 deg] with $S = 4$.

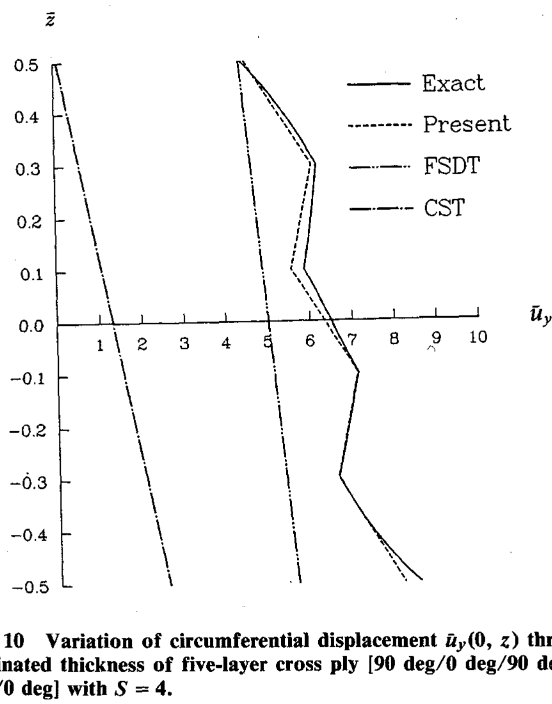

Fig. 10 Variation of circumferential displacement $\bar{u}_y(0, z)$ through laminated thickness of five-layer cross ply [90 deg/0 deg/90 deg/90 deg/0 deg] with $S = 4$.

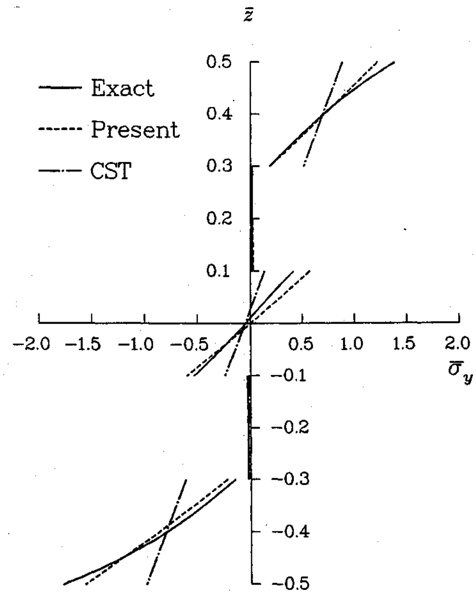

Fig. 11 Variation of circumferential stress $\bar{\sigma}_y(b/2, z)$ through laminated thickness of five-layer cross ply [90 deg/0 deg/90 deg/0 deg/90 deg] with $S = 4$.

Conclusions

A mixed approach for considering the effect of shear deformation for thick multilayered anisotropic shells is presented in this paper. The approach makes use of Jing and Liao's functional with independently assumed displacements and transverse shear stresses. In the present formulation, the number of governing equations is independent of the number of layers. The governing equations for general shells are obtained. From the examples studied here, some conclusions can be made.

1) The present mixed approach works well to model the cylindrical bending behavior of thick shells up to $S = 4$.

2) The zigzag type of assumed displacements is a good approximation even for laminated shells since it can model the zigzag through-thickness behavior of laminated structures.

3) This mixed approach yields more reasonable through-thickness distribution of shear stress for laminated shells as well as for laminated plates. Moreover, it is not necessary to introduce shear coefficients in this approach.

4) Although the zigzag function in addition to the Reissner-Mindlin type of displacements can improve the in-plane response, the bending stresses are still linear. From exact solutions, it is found that the in-plane stresses are nonlinear functions of thickness. The initial curvature effect in strain-displacement relations can make certain improvements in this aspect.

5) The initial curvature effect in stress resultants cannot be neglected for thick shells. Otherwise, when it is combined with the strain-displacement relations, the final stiffness coefficients will be underestimated.

6) In the assumed transverse shear stress field, the contribution from the initial curvature effect is also very important, as can be seen from the stress values at the interfaces and the distributions through the thickness.

Appendix

The coefficients $a_i^{(k)}$, $d_i^{(k)}$, $b_j^{(k)}$, $c_j^{(k)} (j = 1 \sim 4)$, and $e_\alpha^{(k)}$ appearing in Eqs. (13a–13d) are

$$a_1^{(k)} = \frac{9k_1k_2}{4k_2^{(k)2}\,h_k}\,[\tilde{g}_1 - 8\tilde{g}_3 + 16\tilde{g}_5 + \tilde{a}(\tilde{g}_0 - 8\tilde{g}_2 + 16\tilde{g}_4)]$$

$$a_2^{(k)} = \frac{9k_1k_2}{4k_1^{(k)2}\,h_k}\,[\tilde{f}_1 - 8\tilde{f}_3 + 16\tilde{f}_5 + \tilde{b}(\tilde{f}_0 - 8\tilde{f}_2 + 16\tilde{f}_4)]$$

$$a_3^{(k)} = \frac{6k_1k_2}{5k_1^{(k)}k_2^{(k)}h_k}$$

$$b_1^{(k)} = \frac{3k_1k_2h_k}{2k_2^{(k)}}\left(\frac{1}{30} + \frac{\tilde{a}}{3}\right) \qquad b_2^{(k)} = \frac{3k_1k_2h_k}{2k_1^{(k)}}\left(\frac{1}{30} + \frac{\tilde{b}}{3}\right)$$

$$b_3^{(k)} = \frac{3k_1k_2h_k}{2k_2^{(k)}}\left(\frac{-1}{30} + \frac{\tilde{a}}{3}\right) \qquad b_4^{(k)} = \frac{3k_1k_2h_k}{2k_1^{(k)}}\left(\frac{-1}{30} + \frac{\tilde{b}}{3}\right)$$

$$c_1^{(k)} = k_2h_k^2\left(\frac{1}{12} + \frac{\tilde{b}}{2}\right) \qquad c_2^{(k)} = k_1h_k^2\left(\frac{1}{12} + \frac{\tilde{a}}{2}\right) \tag{A1}$$

$$c_3^{(k)} = k_2h_k^2\left(\frac{-1}{12} + \frac{\tilde{b}}{2}\right) \qquad c_4^{(k)} = k_1h_k^2\left(\frac{-1}{12} + \frac{\tilde{a}}{2}\right)$$

$$d_1^{(k)} = k_1k_2h_k^3\left[\frac{1}{30} + \frac{(\tilde{a} + \tilde{b})}{12} + \frac{\tilde{a}\tilde{b}}{3}\right]$$

$$d_2^{(k)} = k_1k_2h_k^3\left(\frac{1}{120} + \frac{\tilde{a}\tilde{b}}{6}\right)$$

$$d_3^{(k)} = k_1k_2h_k^3\left[\frac{1}{30} - \frac{(\tilde{a} + \tilde{b})}{12} + \frac{\tilde{a}\tilde{b}}{3}\right]$$

$$e_1^{(k)} = \frac{k_2}{k_2^{(k)}} \qquad e_2^{(k)} = \frac{k_1}{k_1^{(k)}}$$

where

$$\tilde{f}_0 = \sum_{n=1,2,\ldots}^{\infty} \frac{\tilde{a}^{-2n+1}}{2^{2(n-1)}(2n-1)}, \quad \tilde{f}_1 = \sum_{n=1,2,\ldots}^{\infty} \frac{-\tilde{a}^{-2n}}{2^{2n}(2n+1)}$$

$$\tilde{f}_2 = \sum_{n=1,2,\ldots}^{\infty} \frac{\tilde{a}^{-2n+1}}{2^{2n}(2n+1)}, \quad \tilde{f}_3 = \sum_{n=1,2,\ldots}^{\infty} \frac{-\tilde{a}^{-2n}}{2^{2(n+1)}(2n+3)}$$

$$\tilde{f}_4 = \sum_{n=1,2,\ldots}^{\infty} \frac{\tilde{a}^{-2n+1}}{2^{2(n+1)}(2n+3)}, \quad \tilde{f}_5 = \sum_{n=1,2,\ldots}^{\infty} \frac{-\tilde{a}^{-2n}}{2^{2(n+3)}(2n+5)}$$

$$\tilde{g}_0 = \sum_{n=1,2,\ldots}^{\infty} \frac{\tilde{b}^{-2n+1}}{2^{2(n-1)}(2n-1)}, \quad \tilde{g}_1 = \sum_{n=1,2,\ldots}^{\infty} \frac{-\tilde{b}^{-2n}}{2^{2n}(2n+1)}$$

$$\tilde{g}_2 = \sum_{n=1,2,\ldots}^{\infty} \frac{\tilde{b}^{-2n+1}}{2^{2n}(2n+1)}, \quad \tilde{g}_3 = \sum_{n=1,2,\ldots}^{\infty} \frac{-\tilde{b}^{-2n}}{2^{2(n+1)}(2n+3)}$$

$$\tilde{g}_4 = \sum_{n=1,2,\ldots}^{\infty} \frac{\tilde{b}^{-2n+1}}{2^{2(n+1)}(2n+3)}, \quad \tilde{g}_5 = \sum_{n=1,2,\ldots}^{\infty} \frac{-\tilde{b}^{-2n}}{2^{2(n+3)}(2n+5)} \tag{A1a}$$

where $\tilde{a} = 1/k_1^{(k)}h_k$ and $\tilde{b} = 1/k_2^{(k)}h_k$.

The matrices ℓ_α^T, m_α^T, A_1, B_1, F_1, p_α, and q_α appearing in Eqs. (21) are

$$\ell^T_{1_{1\times N}} = [e_2^{(1)} \ldots e_2^{(N)}], \qquad \ell^T_{2_{1\times N}} = [\lambda_2 e_2^{(1)} \ldots \lambda_2 e_2)^{(N)}]$$

$$m^T_{1_{1\times N-1}} = q_1^T, \qquad m^T_{2_{1\times N-1}} = q_2^T$$

$$A_{1_{N\times N-1}} = \begin{bmatrix} & 0 \\ (b_2/a_2)^{(k)} & (b_4/a_2)^{(k)} \\ 0 & \end{bmatrix}$$

$$F_{1_{N-1\times N}} = \begin{bmatrix} & 0 \\ (S_{22}b_4)^{(k)} & (S_{22}b_2)^{(k+1)} \\ 0 & \end{bmatrix}$$

$$B_{1_{N-1\times N-1}} =$$

$$\begin{bmatrix} & & 0 \\ (S_{22}d_2)^{(k)} & [(S_{22}d_3)^{(k)} + (S_{22}d_1)^{(k+1)}] & (S_{22}d_2)^{(k+1)} \\ 0 & & \end{bmatrix} \quad \text{(A2)}$$

$$p_{1_{N\times 1}} = \left[\left(\frac{e_2}{S_{22}a_2}^{(1)}\right)\cdots\left(\frac{e_2}{S_{22}a_2}\right)^{(N)}\right]^T$$

$$p_{2_{N\times 1}} = \left[\left(\frac{e_2\lambda_2}{S_{22}a_2}^{(1)}\right)\cdots\left(\frac{e_2\lambda_2}{S_{22}a_2}\right)^{(N)}\right]^T$$

$$q_{1_{N-1\times 1}} = \left[c_4^{(1)} + c_2^{(2)}\cdots c_4^{(N-1)} + c_2^{(N)}\right]^T$$

$$q_{2_{N-1\times 1}} = \left[(\lambda_2c_4)^{(1)} + (\lambda_2c_2)^{(2)}\cdots(\lambda_2c_4)^{(N-1)} + (\lambda_2c_2)^{(N)}\right]^T$$

where $\lambda_2^{(k)} = (-1)^k(2/h_k)(1 + z_0^{(k)}/R)$.

The constants $a_2^{(k)}$, $b_2^{(k)}$, $b_4^{(k)}$, $c_2^{(k)}$, $d_1^{(k)}$, $d_2^{(k)}$, $d_3^{(k)}$, and $e_2^{(k)}$ in Eqs. (A2) for cylindrical shells are shown as follows:

$$a_2^{(k)} = \frac{6[R + z_0^{(k)}]}{5Rh_k}, \qquad b_2^{(k)} = \frac{R + z_0^{(k)}}{2R} + \frac{h_k}{20R}$$

$$b_4^{(k)} = \frac{[R + z_0^{(k)}]}{2R} - \frac{h_k}{20R}, \qquad c_2^{(k)} = \frac{h_k}{2}, \qquad c_4^{(k)} = c_2^{(k)}$$

$$d_1^{(k)} = \frac{[R + z_0^{(k)}]h_k}{3R} + \frac{h_k^2}{12R}, \qquad d_2^{(k)} = \frac{[R + z_0^{(k)}]h_k}{6R}$$

$$d_3^{(k)} = \frac{[R + z_0^{(k)}]h_k}{3R} - \frac{h_k^2}{12R}, \qquad e_2^{(k)} = 1$$

The components of matrix V in Eq. (23) are

$$v_{11} = q^2G_{22} + r^2G_{11}^*, \quad v_{12} = -qr(G_{22} + G_{11}^*)$$

$$v_{13} = q^2F_{22} - rG_{11}^*, \quad v_{14} = q^2E_{22} - rG_{12}^*, \quad v_{21} = v_{12}$$

$$v_{22} = q^2G_{11}^* + r^2G_{22}, \quad v_{23} = q(G_{11}^* - rF_{22})$$

$$v_{24} = q(G_{12}^* - rE_{22}), \quad v_{31} = v_{13}, \quad v_{32} = v_{23} \qquad \text{(A3)}$$

$$v_{33} = q^2P_{22} + G_{11}^*, \quad v_{34} = q^2Q_{22} + G_{12}^*$$

$$v_{41} = q^2E_{22} - rG_{21}^*, \quad v_{42} = q(G_{21}^* - rE_{22})$$

$$v_{43} = q^2Q_{22} + G_{21}^*, \quad v_{44} = q^2Z_{22} + G_{22}^*, \quad r = \frac{1}{R}, \quad q = \frac{\pi}{b}$$

References

[1]Reddy, J. N., "A Review of Refined Theories of Laminated Composite Plates," *Shock and Vibration Digest*, Vol. 22, No. 7, 1990, pp. 3–17.

[2]Reddy, J. N., "A General Non-Linear Third-Order Theory of Plates with Moderate Thickness," *Journal of Non-Linear Mechanics*, Vol. 25, No. 6, 1990, pp. 677–686.

[3]Reddy, J. N., "On Refined Theories of Composite Laminates," *Mechanica*, Vol. 25, No. 4, 1990, pp. 230–238.

[4]Noor, A. K., and Burton, W. S., "Assessment of Shear Deformation Theories for Multilayered Composite Plates," *Applied Mechanics Reviews*, Vol. 42, No. 1, 1989, pp. 1–11.

[5]Naghdi, P. M., "A Survey of Recent Progress in the Theory of Elastic Shells," *Applied Mechanics Reviews*, Vol. 9, No. 9, 1956, pp. 365–368.

[6]Ambartsumyan, S. A., "Theory of Anisotropic Shells," NASA TTF-118, 1964.

[7]Zukas, J. A., and Vinson, J. R., "Laminated Transversely Isotropic Cylindrical Shells," *Journal of Applied Mechanics*, Vol. 38, June 1971, pp. 400–407.

[8]Dong, S. B., and Tso, F. K. W., "On a Laminated Orthotropic Shell Theory Including Transverse Shear Deformation," *Journal of Applied Mechanics*, Vol. 39, Dec. 1972, pp. 1091–1096.

[9]Reddy, J. N., "Exact Solutions of Moderately Thick Laminated Shells," *Journal of Engineering Mechanics*, Vol. 110, No. 5, 1984, pp. 794–809.

[10]Khdeir, A. A., Librescu, L., and Frederick, D., "A Shear Deformable Theory of Laminated Composite Shallow Shell-Type Panels and Their Response Analysis II: Static Response," *Acta Mechanica*, Vol. 77, Sept. 1989, pp. 1–12.

[11]Reddy, J. N., and Liu, C. F., "A Higher Order Shear Deformation Theory of Laminated Elastic Shells," *International Journal of Engineering Sciences*, Vol. 23, No. 3, 1985, pp. 319–330.

[12]Dennis, S. T., and Palazotto, A. N., "Laminated Shell in Cylindrical Bending, Two-Dimensional Approach vs Exact," *AIAA Journal*, Vol. 29, No. 4, 1991, pp. 647–650.

[13]Noor, A. K., and Burton, W. S., "Assessment of Computational Models for Multilayered Composite Shells," *Applied Mechanics Reviews*, Vol. 43, No. 4, 1990, pp. 67–97.

[14]Voyiadjis, G. Z., and Shi, G., "A Refined Two-Dimensional Theory for Thick Cylindrical Shells," *International Journal of Solids and Structures*, Vol. 27, No. 3, 1991, pp. 261–282.

[15]Hsu, T. M., and Wang, J. T. S., "A Theory of Laminated Cylindrical Shells Consisting of Layers of Orthotropic Laminae," *AIAA Journal*, Vol. 8, No. 12, 1970, pp. 2141–2146.

[16]Di Sciuva, M., "An Improved Shear-Deformation Theory for Moderately Thick Multilayered Anisotropic Shells and Plates," *Journal of Applied Mechanics*, Vol. 54, Sept. 1987, pp. 589–596.

[17]Murakami, H., "Laminated Composite Plate Theory with Improved In-Plane Responses," *Journal of Applied Mechanics*, Vol. 53, Sept. 1986, pp. 661–666.

[18]Reissner, E., "On a Certain Mixed Variational Theorem and on Laminated Elastic Shell Theory," *Refined Dynamic Theory of Beams, Plates, and Shells*, Springer-Verlag, Berlin, Germany, 1987, pp. 17–27.

[19]Reissner, E., "On a Certain Mixed Variational Theorem and a Proposed Application," *International Journal for Numerical Methods in Engineering*, Vol. 20, 1984, pp. 1366–1368.

[20]Jing, H. S., and Liao, M. L., "Partial Hybrid Stress Element for the Analysis of Thick Laminated Composite Plates," *International Journal for Numerical Methods in Engineering*, Vol. 28, 1989, pp. 2813–2827.

[21]Grigolyuk, E. I., and Kulikov, G. M., "General Direction of Development of the Theory of Multilayered Shells," *Mekhanika Kompozitnykh Materialov*, Vol. 24, No. 2, 1988, pp. 287–298 (English translation in *Mechanics of Composite Materials*, Vol. 24, No. 2, 1988, pp. 231–241).

[22]Jing, H. S., and Tzeng, K. G., "On Two Mixed Variational Principles for Thick Laminated Composite Plates," *Composite Structures* (to be published).

[23]Flügge, W., *Stresses in Shells*, 2nd ed., Springer-Verlag, Berlin, 1973.

[24]Cheng, S., and Ho, B. P. C., "Stability of Heterogeneous Aeolotropic Cylindrical Shells Under Combined Loading," *AIAA Journal*, Vol. 1, No. 4, 1963, pp. 892–898.

[25]Ren, J. G., "Exact Solutions for Laminated Cylindrical Shells in Cylindrical Bending," *Composites Science and Technology*, Vol. 29, No. 3, 1987, pp. 169–187.